A Selectively Activated Extrinsic Cohesive Model

William M. Peterson[1] and Douglas S. Cairns[2]
Montana State University, Bozeman, MT 59717

Fracture simulations are performed using a modified cohesive zone model in which cohesive elements remain dormant until selectively reactivated during the course of an analysis. Prior to the onset of damage, interfacial separation is prevented using controllable multipoint constraints. Cohesive elements may then be dynamically reactivated at critical points within the mesh by releasing the appropriate constraints. Once reactivated, an extrinsic traction-separation law governs the interfacial separation. The method successfully addresses the problem of artificial compliance inherent to the intrinsic cohesive zone model, while activating additional degrees of freedom only as needed to permit crack growth without the need for adaptive remeshing operations.

I. Introduction

IN the cohesive zone model (CZM), zero-thickness cohesive interface elements (CIEs) are placed between standard continuum elements in order to provide a path through which cracks may propagate, as illustrated by Fig. 1. Note that in the initial configuration, corresponding nodes on either side of the interface share the same location. Each CIE in the cohesive zone near a crack tip is governed by a traction-separation law (TSL) that describes the softening or degradation of the material as a function of the normal and tangential separation across an interface, up to the point of failure. A large body of work describing the use and development of the CZM is available in the literature, see for example.[1-7]

In order to clarify the purpose for the modified approach used in this paper, we note that in current practice the CZM is often grouped into two basic approaches. In the first and most common method, referred to as the intrinsic CZM, cohesive elements are initially placed within the mesh prior to obtaining the solution and are an inherent feature of the model. The CIEs are usually positioned along an expected fracture path[8], however in some works the CIEs are placed throughout the mesh at every inter-element boundary in order to permit fracture to occur without prescribing the crack path. This technique is also suitable for modeling multiple crack growth and fragmentation[9,10]. Ideally, the presence of undamaged cohesive elements does not affect the overall response of the structure. However, a consequence of the intrinsic approach is that a small but unavoidable elastic response occurs prior to the onset of damage in each CIE. This results in a mesh-dependent accumulation of additional or "artificial" compliance in the model behavior for a given load condition, particularly in the case where a large number of CIE are present throughout the mesh. The amount of separation allowed prior to the onset of damage may be reduced by defining the initial increasing part of the TSL to be very stiff, such that the element becomes initially nearly rigid.[8,11] For example, the standard bilinear intrinsic TSL shown in Fig. 2 is characterized by three parameters: the initial penalty stiffness, K_0, the critical traction at the onset of damage, T_c, and the critical fracture energy, G_c. In the bilinear model artificial compliance may be controlled by penalizing the initial separation with very large values of K_0. Unfortunately, this practice often leads to ill-conditioning of the system matrix as well as other potential numerical instabilities leading to non-

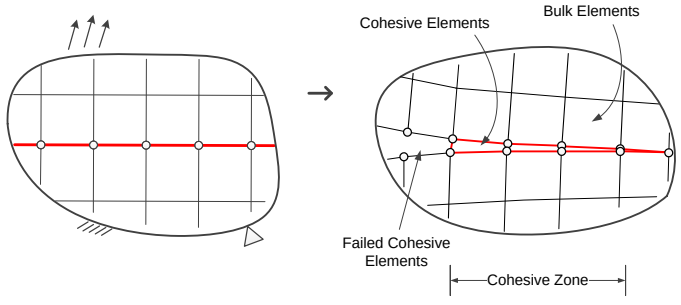

Figure 1. Crack propagation through a cohesive zone using zero-thickness cohesive interface elements.

[1] PhD Candidate, Dept of Mechanical and Industrial Engineering, P.O. Box 173800 Bozeman, MT 59717, AIAA Student Member, william.peterson@msu.montana.edu.
[2] Professor, Dept of Mechanical and Industrial Engineering, P.O. Box 173800 Bozeman, MT 59717, Senior AIAA Member, dcairns@me.montana.edu.

convergence.[12-14] In practice, an acceptable value for a specific analysis is usually found by iteration. Another drawback to the intrinsic approach is the significant number of extra degrees of freedom (DOF) that are introduced when a large number of cohesive elements have been inserted. This issue is somewhat abated by the ease in which the intrinsic CZM can be used with parallel computational methods, provided the necessary hardware is available.

In a second approach known as the extrinsic CZM, cohesive elements are adaptively inserted into the mesh with a non-zero intial traction, T_0, wherever required as the solution progresses.[15,16] The extrinsic TSL is typically defined as a strictly decreasing function of the interface displacement (Fig. 3). Artificial compliance is effectively minimized or eliminated from the global response of the structure, while limiting the increase in the number of active DOF. However, such continual remeshing operations are usually burdened with a significant overhead, and tend to require sophisticated data storage and transfer routines.

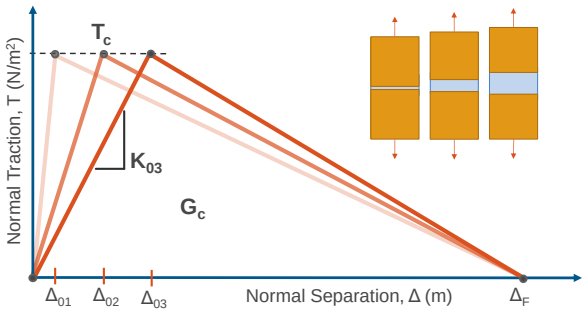

Figure 2. Normal traction component of a standard bilinear intrinsic TSL. *The initial penalty stiffness, K_0, controls the amount of interfacial separation that is allowed to occur prior to the onset of damage.*

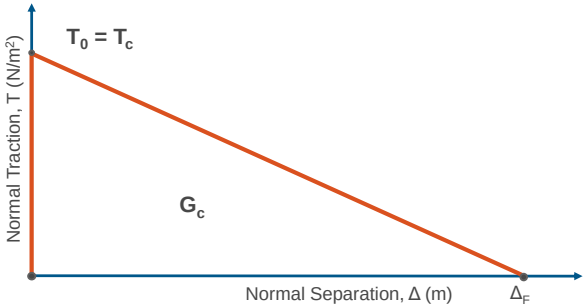

Figure 3. Normal traction component of a linear decreasing extrinsic TSL.

I. MPCs and Selective Activation Strategy

In the current work, we employ a modified cohesive zone model (MCZM) that combines advantages of both intrinsic and extrinsic models. This model is based on the insertion of cohesive elements throughout a mesh prior to an analysis, as in the intrinsic approach. An example intrinsic mesh is shown in Fig. 4. To prevent unwanted interfacial separation, the nodes on either side of each cohesive element are tied using controllable multipoint constraints (Fig. 5). The MPCs may be individually released as the solution proceeds, wherever a criterion has been satisfied. In this way, the method is able to achieve dynamic cohesive element activation, an advantage normally reserved for the extrinsic approach, without requiring the continual overhead of mesh manipulation and storage routines. This is particularly advantageous for parallel computation.

During the insertion process, the mesh is split such that each node that is shared by more than one element is duplicated and the element connectivities updated accordingly. Note that the original and duplicate nodes are defined to have exactly the same (x,y,z)-coordinate location. Furthermore, in our implementation the original nodes are retained in order to retain any loads or boundary conditions applied to the original model before the mesh was split. Each DOF of the duplicate "slave" nodes, u_i^s, are then exactly constrained to the corresponding DOF of the original "master" node, u_i^m, using very simple linear homogenous equations of the form shown in Eq. (1):

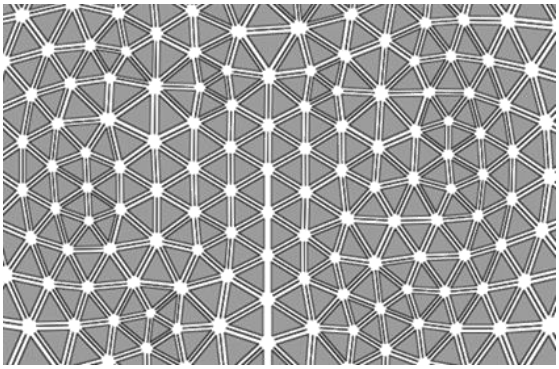

Figure 4. Example intrinsic CZM mesh. *Continuum elements are shrunk in order to indicate the position of the inserted CIEs. A crack is in the center (no CIEs).*

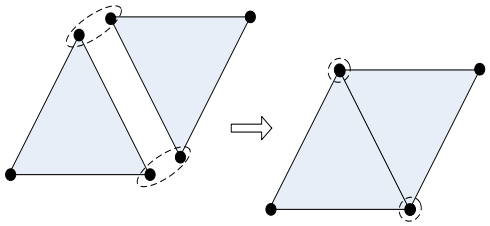

Figure 5. Application of multipoint constraints to prevent interface separation. *Using master-slave DOF elimination, the constrained DOF are eliminated from the system of equations and the CIE lie dormant until the MPCs are removed.*

$$u_i^s = u_i^m \quad \text{for} \quad i = 1,2,\ldots ndof \tag{1}$$

Or, in the canonical form:

$$A_i^s u_i^s + A_i^m u_i^m = 0 \tag{2}$$

Note that in practice, these constraints are usually applied during element assembly. However, the mathematical basis is easily conceptualized by the following explanation. The set of all constraint equations over every DOF in the mesh can be expressed by:

$$\boldsymbol{u}_u + \boldsymbol{A}_s \boldsymbol{u}_s + \boldsymbol{A}_m \boldsymbol{u}_m = \boldsymbol{0} \tag{3}$$

$$\boldsymbol{u}_s = \boldsymbol{0}\boldsymbol{u}_u - \boldsymbol{A}_s^{-1}\boldsymbol{A}_m \boldsymbol{u}_m \tag{4}$$

$$\boldsymbol{u}_s = \boldsymbol{0}\boldsymbol{u}_{\mathrm{u}} + \mathbf{T}\boldsymbol{u}_m \tag{5}$$

Or,

$$\{\boldsymbol{u}_s\} = \left[[\boldsymbol{0}], [\mathbf{T}]\right] \begin{Bmatrix} \{\boldsymbol{u}_u\} \\ \{\boldsymbol{u}_m\} \end{Bmatrix} \tag{6}$$

This transformation may be written for all DOF simultaneously in order to obtain a modified DOF vector that contains only active DOF:

$$\begin{Bmatrix} \{\boldsymbol{u}_u\} \\ \{\boldsymbol{u}_m\} \\ \{\boldsymbol{u}_s\} \end{Bmatrix} = \begin{bmatrix} [\boldsymbol{I}] & [\boldsymbol{0}] \\ [\boldsymbol{0}] & [\boldsymbol{I}] \\ [\boldsymbol{0}] & [\boldsymbol{T}] \end{bmatrix} \begin{Bmatrix} \{\boldsymbol{u}_u\} \\ \{\boldsymbol{u}_m\} \end{Bmatrix} \tag{7}$$

Or,

$$\boldsymbol{u} = \boldsymbol{T}_g \hat{\boldsymbol{u}} \tag{8}$$

Finally, the modified system of equations is determined by:

$$\begin{aligned} \boldsymbol{f} &= \boldsymbol{K}\boldsymbol{u} \\ \mathbf{T}_g^T \boldsymbol{f} &= \mathbf{T}_g^T \boldsymbol{K} \mathbf{T}_g \hat{\boldsymbol{u}} \\ \hat{\boldsymbol{f}} &= \hat{\boldsymbol{K}} \hat{\boldsymbol{u}} \end{aligned} \tag{9}$$

In other words, the final computational mesh has the same structure that it would have had before cohesive elements were inserted, i.e., the same number of active DOF, bandwidth, etc. The eliminated slave DOF are retained in the "real" mesh so that they may be reactivated as needed during the analysis. By virtue of the method, each intrinsic cohesive element enters a "dormant" state and has no effect on the response of the structure until reactivated.

The modified system of equations is then submitted to the solver. During element operations following each iteration, a release criterion (or equivalently, a "reactivation" criterion) at each interface is calculated from the stress in the two adjacent elements. A macro-element-like technique is used in order to calculate and obtain these values and extrapolate them to the integration points of the CIE, as illustrated in Fig. 6. The extrapolated stresses are then rotated into the global coordinate system and averaged. The maximum principal stress and interface tractions are then calculated from the averaged stress and used to evaluate the MPC release criterion. At the end of any converged increment in which a release criterion at a particular CIE has been satisfied, the MPCs constraining the interface nodes are released. Once released, the interface is free to separate in a manner consistent with the intrinsic TSL, or optionally the interface tractions calculated prior to the MPC release can be used as the initial non-zero values in an extrinsic TSL.

This procedure has been implemented in the implicit version of the commercial finite element code, Abaqus/Standard.[17] The key user subroutines used include UEL, MPC, and UFIELD. The current macro-element-based implementation fully supports 2D unstructured meshes consisting of a mix of triangular quadrilateral elements of linear or quadratic order. and work is also underway to extend the approach to three-dimensional models where the reduction in active DOF will be particularly beneficial.

Before closing this section we note that to the best of our knowledge, multipoint constraint-based approaches have been independently developed by a short list of other authors. It appears that the first MPC-based approach was developed by Gerken[18] for regular 2D quadrilateral meshes (interestingly, also implemented via a macro-element-like technique with user subroutines UEL and MPC in Abaqus/Standard), but without the use of a TSL to control subsequent interface separation. Also, a technique very similar to the one used in this paper was described in Ref. (11) as a potential

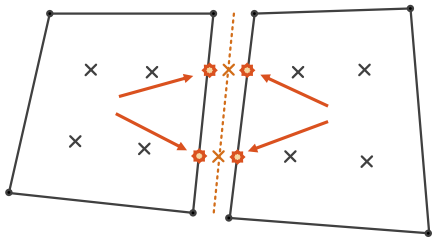

Figure 6. 2D Macroelement. *Stresses are extrapolated from the bordering elements directly to the CIE integration points.*

means to obtain initially rigid cohesive elements, but the author had not yet implemented it. Finally, undamaged cohesive interfaces were constrained in Ref. (19) in an unstructured 2D triangle mesh, and although the authors did not dwell on the details they noted the advantages of the approach in limiting the total number of active DOF and in restricting mesh-dependent artificial compliance.

II. Traction-Separation Law

The interface tractions calculated prior to the MPC release can be used as the initial non-zero values in an extrinsic TSL. An extrinsic TSL defined with respect to a shifted of the origin is used, such that the initial non-zero tractions correspond to a zero opening displacement (see Fig. 7).

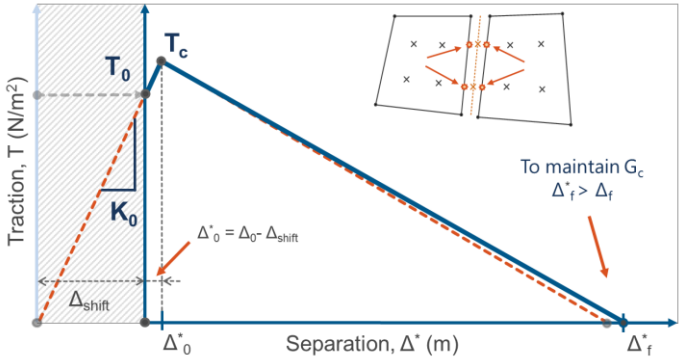

Figure 7. Normal traction component of an extrinsic TSL obtained by shifting a bilinear intrinsic TSL.

III. Examples

A. Ingraffea/Bittencourt Drilled Plate

We take an interesting problem by Ingraffea and Grigoriu,[20] similar to that of Bittencourt et al.,[21] as a test of the selectively activated CZM. In their work, Plexiglas (PMMA) specimens were tested in 3-point bending under the influence of three drilled holes, and the resulting crack path was investigated for various initial crack locations and lengths. We analyze only one of the crack geometries studied by them (Specimen #3), and determine the resulting fracture path for three values of the cohesive fracture energy. A simple displacement-controlled boundary condition was applied to the center of the top edge. The geometry and isotropic material properties are illustrated in Fig. 8. A standard 2D cohesive element available in Abaqus was used without modification of the intrinsic TSL with an initial stiffness of 10·E (in a future publication we will demonstrate an alternative UEL-based cohesive element with an extrinsic TSL). Multipoint constraints were released at an effective Mises stress chosen to be 95% the maximum tensile strength of the material, i.e. $\sigma_{rel} = 0.95*\sigma_{max}$. The original mesh consisted of 58875 nodes, with 19625 3-node plane strain linear triangles and 29223 4-node bilinear cohesive elements. Solutions were obtained between 45-60 mins using 2 cores on a modest Intel i3 with 6GB RAM running Windows 7.

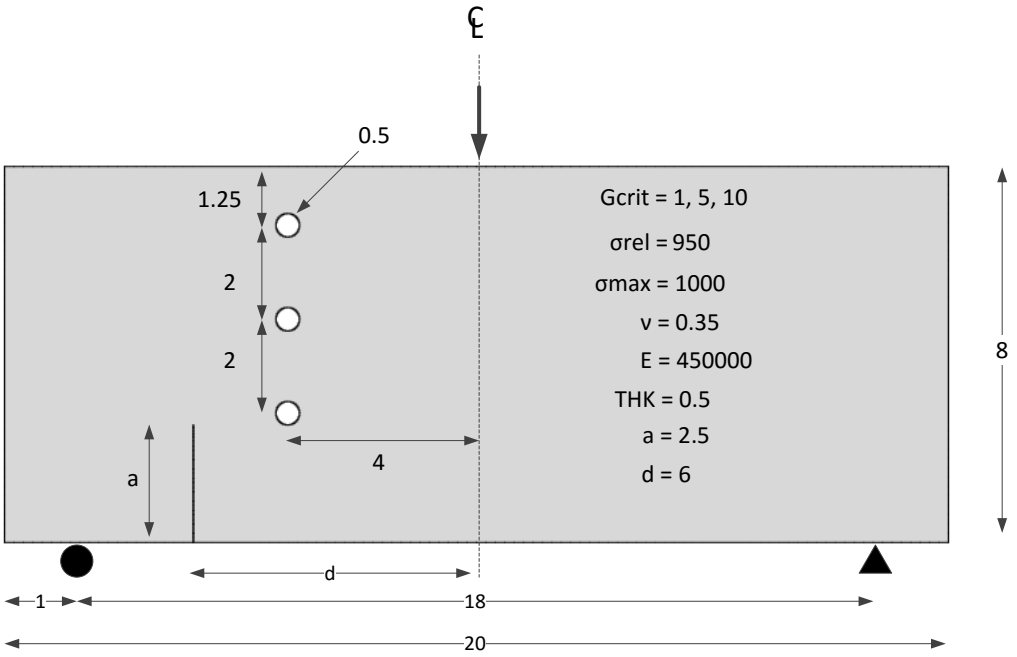

Figure 8. Geometry of Ingraffea/Bittencourt's Drilled Plate Specimen #3. [20,21] *All dims in lbf, inches.*

The crack path results are shown in Figs. 9-11. Dark lines or dots on the interior of the model indicate the presence of a free surface – i.e. an MPC has been released. The results are encouraging, although not exactly the same as in Refs. (20,21). This discrepancy is partly due to the restriction that in our approach crack growth must occur along inter-element boundaries and no attempt at remeshing was made, and partly a result of the simple displacement control method used in our analysis. Also, in order to illustrate a modeling philosophy that accounts for uncertainty in the value used for the fracture energy (or other material properties), for the same mesh, we note the change in the crack path as the critical fracture energy increases.

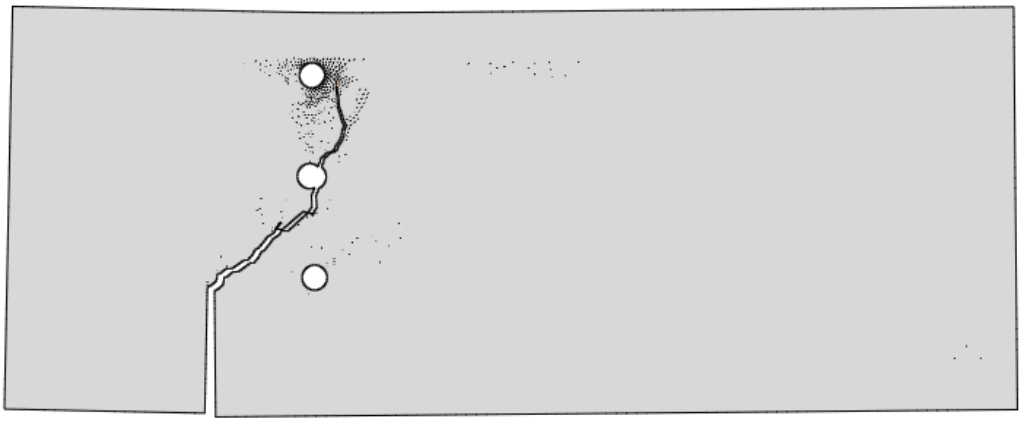

Figure 9. G_{crit} = 10 in-lbf/in^2. *Scale factor=1.*

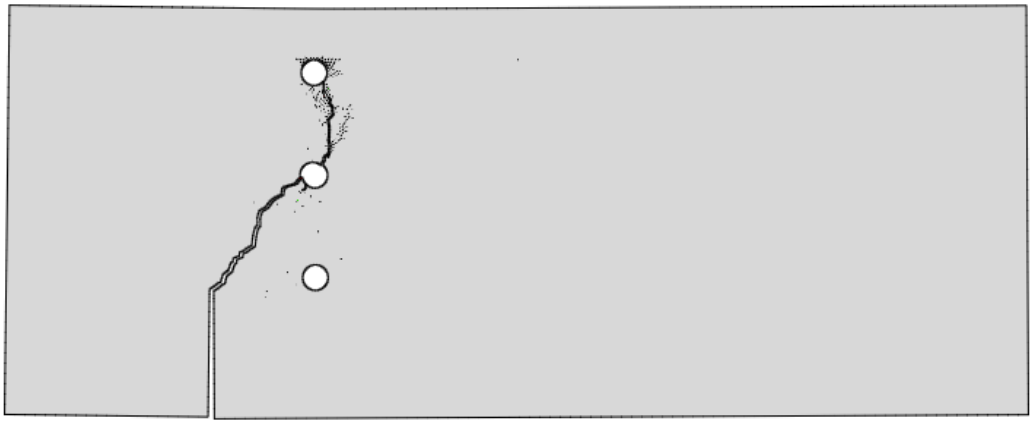

Figure 10. G_{crit} = 5 in-lbf/in^2. *Scale factor=1.*

Figure 11. G_{crit} = 1 in-lbf/in^2. *Scale factor=1.*

IV. Conclusion

The cohesive zone model is a versatile tool for modeling crack initiation and propagation under complex loading conditions, but both intrinsic and extrinsic approaches suffer from some drawbacks. The selective activation of intrinsic cohesive elements appears to be a natural extension that removes or lessens these issues by (1) alleviating the effect of artificial compliance, (2) minimizing the number of DOF in the system matrix while retaining eliminated DOF for reactivation as needed, and (3) utilizing dormant cohesive elements that are selectively reactivated at inter-element boundaries only as needed by the analysis, rather than by interrupting the solution in order to perform adaptive remeshing and element insertion. In the examples given here, it is demonstrated that non-self-similar crack growth can be effectively achieved without prescribing the crack path *a priori*. This is important in the very common case where damage or manufacturing flaws exist within a material, as the evolution of damage can be significantly affected by their presence. Continued development will be reported in future publications.

References

[1]Woo, K. W., Peterson, W. M., and Cairns, D. S., "Selective Activation of Intrinsic Cohesive Elements," *Journal of Applied Mathematics and Physics*, Vol. 2, No. 12, 25 Nov. 2014, pp. 1061-1068. http://dx.doi.org/10.4236/jamp.2014.212121

[2]Dugdale, D. S., "Yielding of Steel Sheets Containing Slits," *Journal of the Mechanics and Physics of Solids*, Vol. 8, No. 2, May 1960, pp. 100-108. http://dx.doi.org/10.1016/0022-5096(60)90013-2

[3]Barenblatt, G. I., "The Mathematical Theory of Equilibrium Cracks in Brittle Fracture," *Advances in Applied Mechanics*, Vol. 7, 1962, pp. 55-129. http://dx.doi.org/10.1016/S0065-2156(08)70121-2

[4]Hillerborg, A., Modeer, M., Petersson, P. E., "Analysis of Crack Formation and Crack Growth in Concrete by Means of Fracture Mechanics and Finite Elements," *Cement and Concrete Research*, Vol. 6, 1976, pp. 773-782. http://dx.doi.org/10.1016/0008-8846(76)90007-7

[5]Ortiz, M., Suresh, S., "Statistical Properties of Residual Stresses and Intergranular Fracture in Ceramic Materials," ASME *Journal of Applied Mechanics*,Vol. 60, No. 1, March 1993, pp. 77-84. http://dx.doi.org/10.1115/1.2900782

[6]Turon, A., Camanho, P. P., Costa, J., Renart, J., "Accurate Simulation of Delamination Growth Under Mixed-Mode Loading Using Cohesive Elements: Definition of Interlaminar Strengths and Elastic Stiffness," *Composite Structures*, Vol. 92, No. 8, July 2010, pp. 1857-1864. http://dx.doi.org/10.1016/j.compstruct.2010.01.012
[7]Kubair, D. V., Geubelle, P. H., "Comparitive Analysis of Extrinsic and Intrinsic Cohesive Models of Dynamic Fracture," *International Journal of Solids and Structures*, Vol. 40, No. 15, July 2003, pp. 3853-3868. http://dx.doi.org/10.1016/S0020-7683(03)00171-9
[8]Alfano, G., Crisfield, M. A., "Finite Element Interface Models for the Delamination Analysis of Laminated Composites: Mechanical and Computational Issues," *International Journal for Numerical Methods in Engineering*, Vol. 50, No. 7, Mar 2001, pp. 1701-1736. http://dx.doi.org/10.1002/nme.93
[9]Xu, X. P., Needleman, A., "Numerical Simulations of Fast Crack Growth in Brittle Solids," *Journal of the Mechanics and Physics of Solids*, Vol. 42, No. 9, 1994, pp. 1397-1434. http://dx.doi.org/ 10.1016/0022-5096(94)90003-5
[10]Miller, O., Freund, L. B., Needleman, A., "Energy Dissipation in Dynamic Fracture of Brittle Materials," *Modelling and Simulation in Materials Science and Engineering*, Vol. 7, No. 4, 1999, ppp. 573-586. http://dx.doi.org/10.1088/0965-0393/7/4/307
[11]Zavattieri, P. D., "Study of dynamic crack branching using intrinsic cohesive surfaces with variable initial elastic stiffness," GM R&D-9650, Aug. 2003.
[12]Gao, Y. F., and Bower, A. F., "A Simple Technique for Avoiding Convergence Problems in Finite Element Simulations of Crack Nucleation and Growth on Cohesive Interfaces," *Modelling and Simulation in Materials Science and Engineering*, Vol. 12, No. 3, May 2004, pp. 453–463. http://dx.doi.org/10.1088/0965-0393/12/3/007
[13]Goyal, V. K., Johnson, E. R., and Dávila, C. G., "Irreversible Constitutive Law for Modeling the Delamination Process Using Interfacial Surface Discontinuities," *Composite Structures*, Vol. 65, Sep. 2004, pp. 289–305. http://dx.doi.org/10.1016/j.compstruct.2003.11.005
[14]Gustafson, P. A., and Waas, A. M., "Efficient and Robust Traction Laws for the Modeling of Adhesively Bonded Joints," *49th AIAA/ASME/ASCE/AHS/ASC Structures, Structural Dynamics, and Materials Conference*, AIAA, Washington, DC, 2008, Paper 2008-1849.
[15]Camacho G. T., Ortiz, M., "Computational Modelling of Impact Damage in Brittle aterials," *International Journal of Solids and Structures Structures*, Vol. 33, No. 22-23, 1996, pp. 2899–2938. http://dx.doi.org/10.1016/0020-7683(95)00255-3
[16]Zhang, Z. J., Paulino, G. H., and Celes, W., "Extrinsic Cohesive Modelling of Dynamic Fracture and Microbranching Instability in Brittle Materials," *International Journal for Numerical Methods in Engineering*, vol. 72, 2007, pp. 893–923. http://dx.doi.org/10.1002/nme.2030
[17]Abaqus, FEA Software Package, Ver. 6.12, Simulia, Dassault Systemes, Providence, RI.
[18]Gerken, J. M., "An Implicit Finite Element Method for Discrete Dynamic Fracture," Master's Thesis, Department of Mechanical Engineering, Colorado State University, Fort Collins, 1999.
[29]Verhoosel, C. V., and Gutiérrez, M. A., "Modelling inter- and transgranular fracture in piezoelectric polycrystals," *Engineering Fracture Mechanics*, Vol. 76, No. 6, Apr. 2009, pp. 742–760. http://dx.doi.org/10.1016/j.engfracmech.2008.07.004
[20]Ingraffea, A. R., Grigoriu, M., "Probabilistic Fracture Mechanics: A Validation of Predictive Capability," AFOSR Report 90-8, Aug. 1990.
[21]Bittencourt, T. N., Wawrzynek, P. A., Ingraffea, A. R., "Quasi-automatic Simulation of Crack Propagation for 2D LEFM Problems," *Engineering Fracture Mechanics*, Vol. 55, No. 2, 1996, pp. 321-334.